Resource

Cell

A Genome-wide RNAi Screen for Modifiers of the Circadian Clock in Human Cells

Eric E. Zhang,[1,2,5] Andrew C. Liu,[1,3,5] Tsuyoshi Hirota,[1,2,5] Loren J. Miraglia,[1] Genevieve Welch,[1] Pagkapol Y. Pongsawakul,[2] Xianzhong Liu,[1] Ann Atwood,[2] Jon W. Huss III,[1] Jeff Janes,[1] Andrew I. Su,[1] John B. Hogenesch,[4,*] and Steve A. Kay[2,*]

[1]Genomics Institute of the Novartis Research Foundation, San Diego, CA 92121, USA

[2]Section of Cell and Developmental Biology, Division of Biological Sciences, University of California, San Diego, La Jolla, CA 92093-0130, USA

[3]Department of Biology, The University of Memphis, Memphis, TN 38152, USA

[4]Department of Pharmacology, Institute for Translational Medicine and Therapeutics, Penn Genome Frontiers Institute, University of Pennsylvania School of Medicine, Philadelphia, PA 19104-6160, USA

[5]These authors contributed equally to this work

*Correspondence: hogenesc@mail.med.upenn.edu (J.B.H.), skay@ucsd.edu (S.A.K.)

DOI 10.1016/j.cell.2009.08.031

SUMMARY

Two decades of research identified more than a dozen clock genes and defined a biochemical feedback mechanism of circadian oscillator function. To identify additional clock genes and modifiers, we conducted a genome-wide small interfering RNA screen in a human cellular clock model. Knockdown of nearly 1000 genes reduced rhythm amplitude. Potent effects on period length or increased amplitude were less frequent; we found hundreds of these and confirmed them in secondary screens. Characterization of a subset of these genes demonstrated a dosage-dependent effect on oscillator function. Protein interaction network analysis showed that dozens of gene products directly or indirectly associate with known clock components. Pathway analysis revealed these genes are overrepresented for components of insulin and hedgehog signaling, the cell cycle, and the folate metabolism. Coupled with data showing many of these pathways are clock regulated, we conclude the clock is interconnected with many aspects of cellular function.

INTRODUCTION

Circadian rhythms in mammals are exemplified by the sleep/wake cycle and regulated by an internal timing system. A central clock in the suprachiasmatic nuclei (SCN) of the hypothalamus coordinates input and, through a complex signaling cascade, synchronizes local clocks in the brain and throughout the body (Reppert and Weaver, 2002; Panda et al., 2002b; Liu et al., 2007a). Over the past two decades, extensive genetic, genomic, molecular, and cell biological approaches identified more than a dozen clock genes that collectively comprise a biochemical feedback loop that drives circadian oscillations (Reppert and Weaver, 2002; Panda et al., 2002b).

Recent models consider the clock a biochemical and cellular oscillator, and also a genetic network. A highly conserved negative feedback loop was discovered and elucidated at biochemical, cellular, and organismal levels in mammals and *Drosophila*; transcription factors play a prominent role in the clock mechanism. The bHLH-PAS transcriptional activators BMAL1 (official name: ARNTL, an ortholog of the *Drosophila cyc* gene) and its heterodimeric partner CLOCK (an ortholog of the *Drosophila Clk* gene) interact to bind to E-box *cis* elements present in the promoter regions of their target genes. These targets include two families of repressor proteins, the PERIODs (PER1, PER2, and PER3) and the CRYPTOCHROMEs (CRY1 and CRY2), which interact in a protein complex that translocates from the cytoplasm to the nucleus. In the nucleus, this repressor complex physically associates with the BMAL1-CLOCK complex to inhibit E-box-mediated transcription. This process results in the cyclic transcription of these repressor genes, as well as thousands of transcriptional output genes elsewhere in the genome (Hughes et al., 2009; Panda et al., 2002a; Ueda et al., 2002).

In addition to rhythmic transcription, PER and CRY protein levels and subcellular localization also oscillate. Protein level cycling is a consequence of the transcriptional regulation mentioned above, but also through posttranscriptional and posttranslational mechanisms that regulate the stability and degradation of messages and proteins. These processes are mediated by kinases (e.g., CSNK1D, CSNK1E, CSNK2, and GSK3B) (Vanselow et al., 2006; Maier et al., 2009; Hirota et al., 2008; Etchegaray et al., 2009) and the proteasomal machinery, including the E3 ligase, FBXL3 (Siepka et al., 2007; Busino et al., 2007; Godinho et al., 2007; Reddy et al., 2006). Thus, while transcriptional regulation generates rhythmic RNA levels, regulated posttranslational modifications control protein abundance, subcellular localization, and repressor activity of PER and CRY.

Importantly, these additional regulatory steps introduce a delay, critical for rhythm generation and period regulation, in the clock mechanism (Gallego and Virshup, 2007).

The circadian oscillator is also a highly interconnected genetic network that uses other transcription factors and response elements. In addition to the biochemical feedback loop that regulates cycling at the E-box (termed the ''core loop''), circadian gene expression is mediated by transcription at the ROR/REV-ERB (RORE) and the DBP/E4BP4 (D-box) binding elements. Two subfamilies of nuclear hormone receptors, the NR1Ds (NR1D1 and NR1D2, or REV-ERBα and β) and RORs (α, β and γ, or RORa, RORb and RORc), either repress or activate gene transcription from the ROR elements in several clock genes (Ukai-Tadenuma et al., 2008). The bZIP transcription factors, DBP, TEF, and HLF, perform similar functions on the D-box element (Gachon et al., 2006).

The role of these genes was examined in vivo and in vitro. Knockout mice for *Rev-erb*α, *Ror*α, or *Ror*β, have lower amplitude rhythms, abnormal period lengths, and interindividual variability in both phenotypes (Andre et al., 1998; Preitner et al., 2002; Sato et al., 2004). A coactivator shown to interact with the ROR proteins, PGC1α, modulates *Bmal1* expression, and *Pgc1*α knockout mice display long-period locomotor activity behavior (Liu et al., 2007c). Furthermore, dose-dependent knockdown of *ROR* and *REV-ERB* genes in vitro has a potent effect on the baseline and the amplitude of circadian gene expression (Baggs et al., 2009). Taken in sum, these data demonstrate the important role of the clock gene network in regulating circadian amplitude, resistance to perturbation, and, in several cases, modulation of period length.

Although the clock *can* function in a cell-autonomous manner (for discussion purposes, we extend the definition of autonomy to include potential auto regulation in *trans*), in vivo rhythms in physiology and behavior result from more complex cellular and humoral interactions. Genetic dissection of the circadian system showed the important role of intercellular coupling in generating physiological and behavioral responses; these explain the apparent discordance among observations from cells, organotypic SCN cultures, and whole animals (Liu et al., 2007b). For example, although *Cry1* deletion in mice causes short period length of locomotor activity rhythms, dissociated SCN neurons and peripheral cells derived from these mice are arrhythmic (Liu et al., 2007b). These results demonstrate that intercellular coupling in the SCN compensates for the loss of *Cry1* function and, as a result, masks the more severe cellular clock deficits. Similarly, while *Clock* gene knockout mice are nearly wild-type in their behavioral rhythms, lung and liver preparations from these mice display arrhythmic gene expression (DeBruyne et al., 2006, 2007). In fact, cellular clock defects are often more severe than behavioral in clock gene knockout mice (Brown et al., 2005; Liu et al., 2007b). Thus, although transcriptional rhythms are cell autonomous and reflect the cellular nature of the circadian signaling, physiology and behavior result from more complex in vivo interactions.

The circadian research community took nearly four decades to identify the above clock components. In metazoan models, successful approaches included forward mutagenesis in flies and mice and cellular and biochemical methods followed by confirmatory reverse genetics. Although these efforts were fruitful, they remain incomplete because evidence, including quantitative trait loci (QTL) studies, suggests that additional clock components and modulators exist (Takahashi, 2004).

Remarkably, circadian clocks exist in cell lines (Balsalobre et al., 1998). Some of these lines are amenable to complementary DNA (cDNA) overexpression and RNA interference (RNAi) techniques and have been used to identify new components of many signal transduction pathways (for example, see Conkright et al., 2003; Iourgenko et al., 2003; Aza-Blanc et al., 2003). To conduct a whole-genome screen for circadian clock modifiers, we used the U2OS (human osteosarcoma) cell line that was successfully employed in chemical screens (Hirota et al., 2008), in dissection of network properties of the oscillator (Baggs et al., 2009), and in a limited-scale RNAi screen (Maier et al., 2009). We screened ~90,000 individual small interfering RNAs (siRNAs) and measured luciferase reporter gene expression every 2 hr for 4 days. We applied statistical algorithms to find modifiers of rhythm amplitude and period length. Knockdown of nearly 1000 genes reduced rhythm amplitude. On the other hand, knockdown of hundreds of genes by multiple independent siRNAs generated strong circadian phenotypes. Characterization of a subset of these genes demonstrated a dosage-dependent effect on clock function. Protein interaction network analysis indicated that some candidates directly or indirectly interact with known clock components. Gene expression studies showed that some affect the clock by regulating clock component expression levels. Finally, to disseminate this data and integrate with existing public resources, we constructed a database (http://biogps.gnf.org/circadian/). This resource will serve the research community in genetic and biochemical investigations of circadian regulation of physiology and behavior.

RESULTS

Assay Development

Because circadian rhythms are dynamic, we employed kinetic, rather than steady-state, bioluminescence detection to assess the persistence and characteristics of rhythms after perturbation. To conduct such a screen, we required a cell line amenable to efficient reverse transfection, where siRNAs are deposited on plates, dried, mixed with transfection reagents and, finally, cells are added to complete the transfection process. We chose U2OS cells for assay development as this model was extensively characterized by functional studies examining knockdown effects of all known clock components with cellular and behavioral phenotypes in knockout mice (Baggs et al., 2009; Liu et al., 2007b). In addition, this model was used in small molecule screening and limited-scale RNAi screening to find modifiers of amplitude and periodicity (Hirota et al., 2008; Maier et al., 2009; Baggs et al., 2009).

We established cell lines harboring a rapidly degradable form of luciferase, *dLuc*, driven by the mouse *Bmal1* or *Per2* gene promoter (Liu et al., 2008) (Figure S1 available online). Knockdown of *CRY1*, *CRY2*, and *BMAL1* in both lines resulted in phenotypes consistent with previous knockout mouse and cellular knockdown studies (Liu et al., 2007b, 2008; Maier et al., 2009; Baggs et al., 2009) (Figure S1). For instance, *CRY1*

knockdown shortens period length and compromises rhythm persistence, *CRY2* knockdown lengthens period length, and knockdown of both results in arrhythmicity.

We next adapted these assays for high-throughput screening (HTS) in 96- and 384-well plates. By optimizing growth conditions and transfection efficiency, we obtained consistent bioluminescence rhythms in a HTS format (e.g., ± 0.5 hr of SD in control wells of 384-well plates, n = 7680 wells) with knockdown effects for period and amplitude (see below). Knockdown of known clock components such as *CRY1*, *CRY2*, and *BMAL1* in this format produced similar cellular clock phenotypes to those in LumiCycle assays using 35 mm dishes (Figure S1). These conditions enabled large-scale siRNA screens.

Primary Screen

The screening protocol and logic are outlined in Figures 1A and S2 and describe the primary screen, data mining, hit selection, secondary screen, and validation studies. The *Bmal1-dLuc* line was more robust than our *Per2-dLuc* line and therefore was used for primary screens in a 384-well format. *CRY2* siRNAs were used as positive controls in each plate. We screened an siRNA library (QIAGEN) targeting 17,631 known and 4837 predicted human genes. In these libraries, four siRNA constructs were designed for each gene with a pool of two siRNAs per well (two siRNAs/well, two wells/gene) for a total of 89,872 siRNAs. These siRNAs were prespotted on 384-well plates. After addition of transfection reagent, we seeded approximately 2000 cells into each well to complete the transfection. We measured bioluminescence every 2 hr for 4 days for a total of 48 time points for each well; this temporal resolution was chosen based on simulation studies using data collected from known clock gene perturbation. The primary screen produced a total of >4.3 × 10^6 data points, which are also deposited in the PubChem Bioassay database (accession number AID 1904; see the Experimental Procedures for details).

Data Mining

We used the MultiCycle Analysis program (Actimetrics) to analyze period length and rhythm amplitude for each well. Plate-to-plate variation in period length and amplitude was modest in control wells (period length or τ = 25.20 hr ± 0.55 [mean ± SD], n = 1176; amplitude or A = 4380 ± 1010, n = 1176) (Figures 1B and S3). Knockdown of *CRY2*, a period length control, resulted in robust lengthening (29.43 hr ± 0.65; n = 1176), while knockdown of *BMAL1*, an amplitude control, potently reduced amplitude (692 ± 626 arbitrary luminescence units; n = 1176).

Gratifyingly, many known clock components had phenotypes in this screen consistent with those seen in knockout animals (Liu et al., 2007b; Liu et al., 2008) or dose-dependent siRNA knockdown (Baggs et al., 2009) (Figure 1C). For example, *CRY2* knockdown lengthened period, and *CRY1* knockdown led to rapid loss of rhythmicity. Knockdown of *BMAL1* or *CLOCK* genes resulted in low amplitude/arrhythmicity, and knockdown of *PER1* or *PER2* also caused almost immediate arrhythmicity. Consistent with its role as a repressor for RORE-mediated transcription, knockdown of *NR1D1* raised overall reporter expression levels and lengthened the period (see below), consistent with a previous report (Baggs et al., 2009). We also saw knockdown effects for *CSNK1D* and *CSNK1E* (Xu et al., 2005; Meng et al., 2008; Gallego and Virshup, 2007; Etchegaray et al., 2009), *GSK3B* (Hirota et al., 2008), *FBXL3* (Siepka et al., 2007; Busino et al., 2007; Godinho et al., 2007), *FBXW11* (or *β-TRCP2*), and *CSNK2* (Maier et al., 2009). Collectively, these results support the suitability of our primary screen.

Primary Hit Selection

To identify genes whose knockdown modulates the circadian clock, rather than the overall health of the cells, we focused on period length deficits and increased amplitude of rhythmicity. Low-amplitude traces usually exhibit poor curve fitting and generate inconsistent period length data between replicate wells; they constitute less than 4.5% of all wells and were excluded from the analysis (Figure S4). We found 1028 short-period hits, including 76 genes that were hit by two independent siRNA pairs (double hits), 4230 long-period hits (274 double hits), and 493 high-amplitude hits (18 double hits) (Figure 1B). Consistent with data from small molecule screens (Hirota et al., 2008) (T.H and S.A.K., unpublished data) and previous model organism screens (Takahashi, 2004), many more genes generated long period length than short.

As siRNAs have well described potential "off target" effects, we focused on genes where two or more independent siRNAs generated a consistent phenotype (Echeverri et al., 2006). The plotted traces for these genes were individually inspected to remove false positives caused by poor curve fitting. We selected 254 genes whose knockdown resulted in strong circadian phenotypes, defined by three or more standard deviations from the mean, in period length and rhythm amplitude (Figure S2). We also selected 89 single siRNA pair hits that showed strong circadian phenotypes in duplicate wells (Figure S2). Thus, our primary hit selection list contains a total of 343 genes including known clock components (Table S1 and Figure 1).

Secondary Confirmation Screen

Next, we performed a secondary screen to confirm the knockdown phenotypes identified in the primary screen (Figure S2). We tested at least four siRNA constructs (one siRNA/well, at least four wells/gene) for each gene in both the *Bmal1-dLuc* and *Per2-dLuc* reporter cell lines (Figure S1). We hypothesized that consistent changes in both assays indicate that resultant phenotype is not reporter or response element specific, but rather reports an impact on clock function in cells.

As expected, the secondary screen using a *Bmal1-dLuc* reporter assay generated highly concordant results with the primary screen (Figures 2A and S2): 222 of 238 genes that were identified in the primary screen with two siRNA pairs and 47 of 83 with a single siRNA pair were confirmed (Table S1). In *Per2-dLuc* reporter assay, 219 were also independently confirmed (Figures 2B–2D and S2). The remaining unconfirmed genes either failed to have more than one independent siRNA conferring a consistent phenotype or confirmed in the *Bmal1-dLuc* but not the *Per2-dLuc* assay. In addition, a few genes altered both period length and amplitude in these assays (Figure S2). In summary, we observed a high level of concordance between our primary and secondary screens, and we

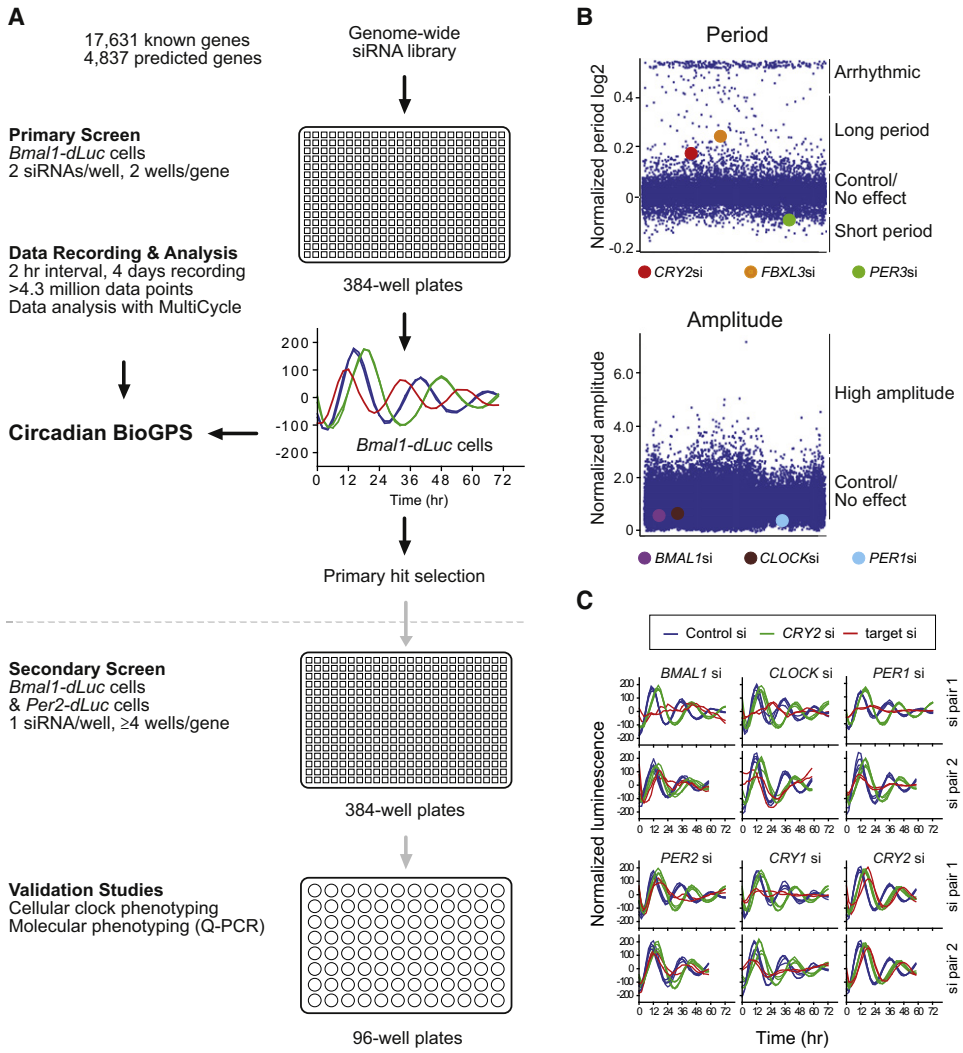

Figure 1. A Cell-Based Genome-wide siRNA Screen for Circadian Clock Modifiers

(A) A schematic diagram of the genome-wide siRNA screen including the primary screen, data mining, hit selection, secondary screen, and validation of several selected targets. In the primary screen, reporter cells were transfected with siRNA in 384-well plates followed by kinetic bioluminescence recording (see the Experimental Procedures for details). Luminescence data were analyzed to obtain circadian parameters and select primary hits. Secondary screen and validation studies were performed to confirm circadian phenotypes of hits and to demonstrate the validity of the primary screen. To catalyze the use of this dataset by the research community, we constructed a comprehensive circadian genomic screen database in BioGPS (see Figure S6 for details).

(B) Distribution of circadian parameters of the entire primary screen. Dots represent normalized period (upper) and amplitude values (lower). For period length, the average of duplicate wells was divided by the mean of the entire screen and indicated in Log2 space. The cutoff was −0.1 and +0.1 (corresponding to raw data 23.55 hr for short- and 26.85 hr for long-period hits). Traces that lack apparent ~24 hr bioluminescence oscillation usually returned as a period length of 48 hr and are considered as arrhythmic. In addition, Log2 values above 0.4 (corresponding to 38 hr), for example, display poor curve fitting and are also considered as arrhythmic. For rhythm amplitude, average of duplicate wells was divided by the mean of the entire screen, and the cutoff was 2.20 (corresponding to raw data 7390) for high-amplitude hits. The knockdown phenotypes of several representative clock genes are shown in colored dots.

(C) Cellular clock phenotypes of siRNA knockdown of known clock genes. Plots of cellular oscillations upon knockdown of *BMAL1*, *CLOCK*, *PER1*, *PER2*, *CRY1*, or *CRY2* by two independent pairs of siRNAs in the primary screen are presented. The spikes of initial 10 hr bioluminescence readings resulted from media change and were removed from the plot.

identified hundreds of genes whose knockdown generates strong circadian phenotypes.

Dose-Dependent Phenotypic Validation

To determine those genes that most sensitively impacted period length or increased amplitude (cellular rheostats of clock function), we conducted a dosage-dependent knockdown analysis as per our previous work (Baggs et al., 2009). In this study, we selected 17 genes from the primary screen with extreme phenotypes and generated an eight-point dose response. All but one showed dose-dependent effects on circadian rhythms (Figure 3A). Gene knockdown was confirmed by quantitative PCR

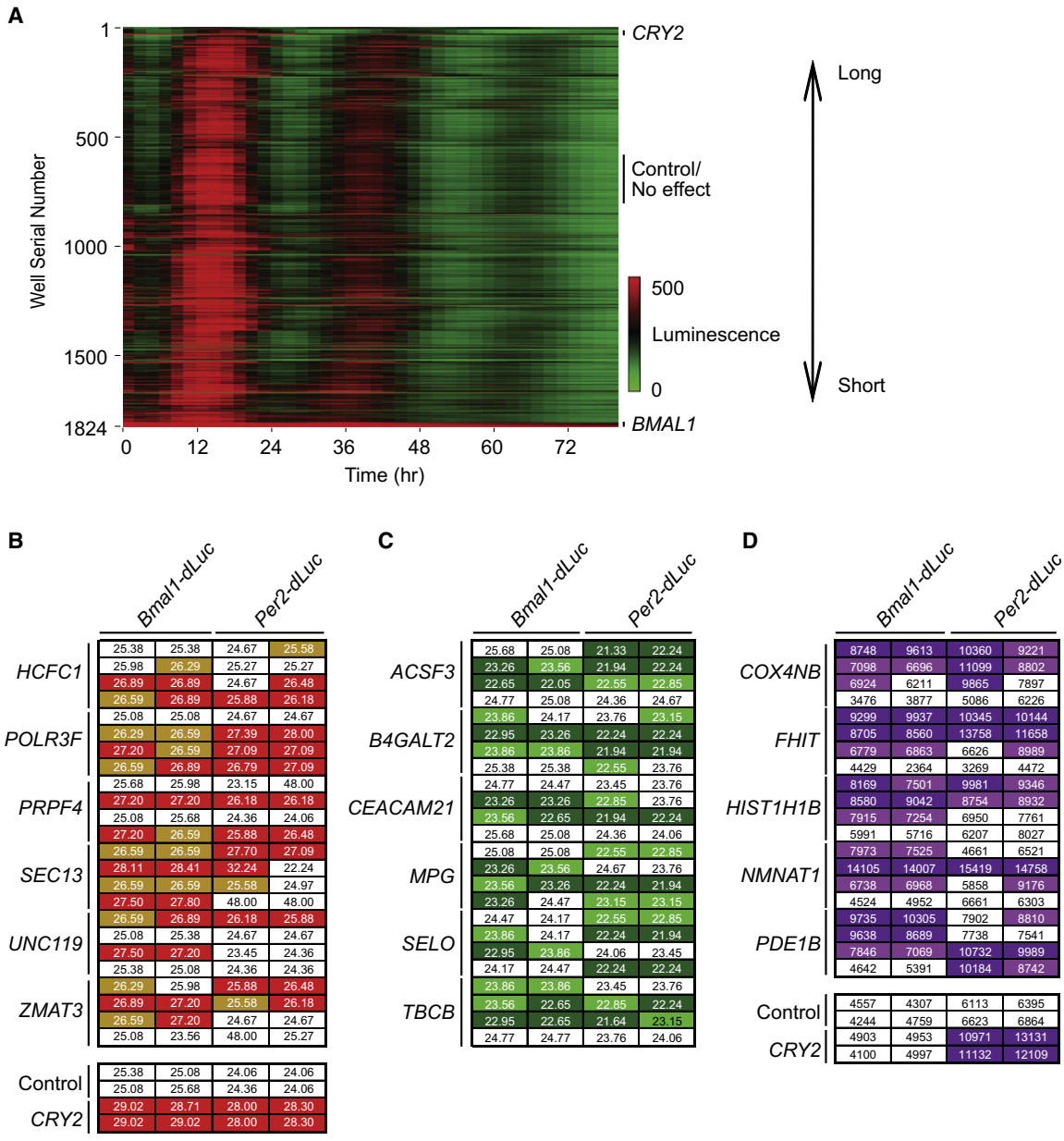

Figure 2. Secondary Confirmation Assay of Cellular Clock Phenotypes

(A) A heat map of the secondary screen using *Bmal1-dLuc* cells. Eight hundred and seventy-two independent siRNAs were tested against 154 genes in duplicate, along with 20 wells for each of the controls (GL2, *CRY2*, *BMAL1*, and GL3 siRNAs) for a total of 1824 wells. Bioluminescence intensity for each well was plotted against time (hr), with each horizontal line representing luminescence recordings from a single well. The circadian profiles from each well were classified by hierarchical clustering (clustering method: maximum complete linkage; similarity measure: correlation; ordering function: average value).

(B–D) Circadian parameters for 17 genes generating long-period (B), short-period (C), and high-amplitude phenotypes (D) in both *Bmal1-dLuc* and *Per2-dLuc* cell lines. *CRY2* siRNA was a positive control. For the *Bmal1-dLuc* cell line, the period length of the control wells was 25.07 hr ± 0.59 and amplitude was 4120 ± 1285 (mean ± SD; n = 768). For the *Per2-dLuc* cell line, the period length was 24.18 hr ± 0.55 and amplitude was 6438 ± 1140 (n = 768). Cellular clock phenotypes are color coded, with darker colors in each category representing stronger alteration of circadian parameters (mean ± 3 × SD) than lighter colors (mean ± 2 × SD). Four different siRNAs (y axis) were tested for each gene, and the assay was conducted in duplicates (x axis) in each screen using either *Bmal1-dLuc* or *Per2-dLuc* cells.

(Q-PCR) (Figure 3B). Genes whose knockdown lengthened period included *HCFC1*, *POLR3F*, *PRPF4*, *SEC13*, *UNC119*, and *ZMAT3*, similar to *CRY2* or *FBXL3*. Knockdown of *ACSF3*, *B4GALT2*, *CEACAM21*, *TBCB*, or *MPG* led to dose-dependent period shortening, similar to *CRY1*. Finally, knockdown of *COX4NB*, *FHIT*, *HIST1H1B*, *NMNAT1*, or *PDE1B* caused dose-dependent increases in rhythm amplitude. These data confirm primary screening results and show that many genes from our

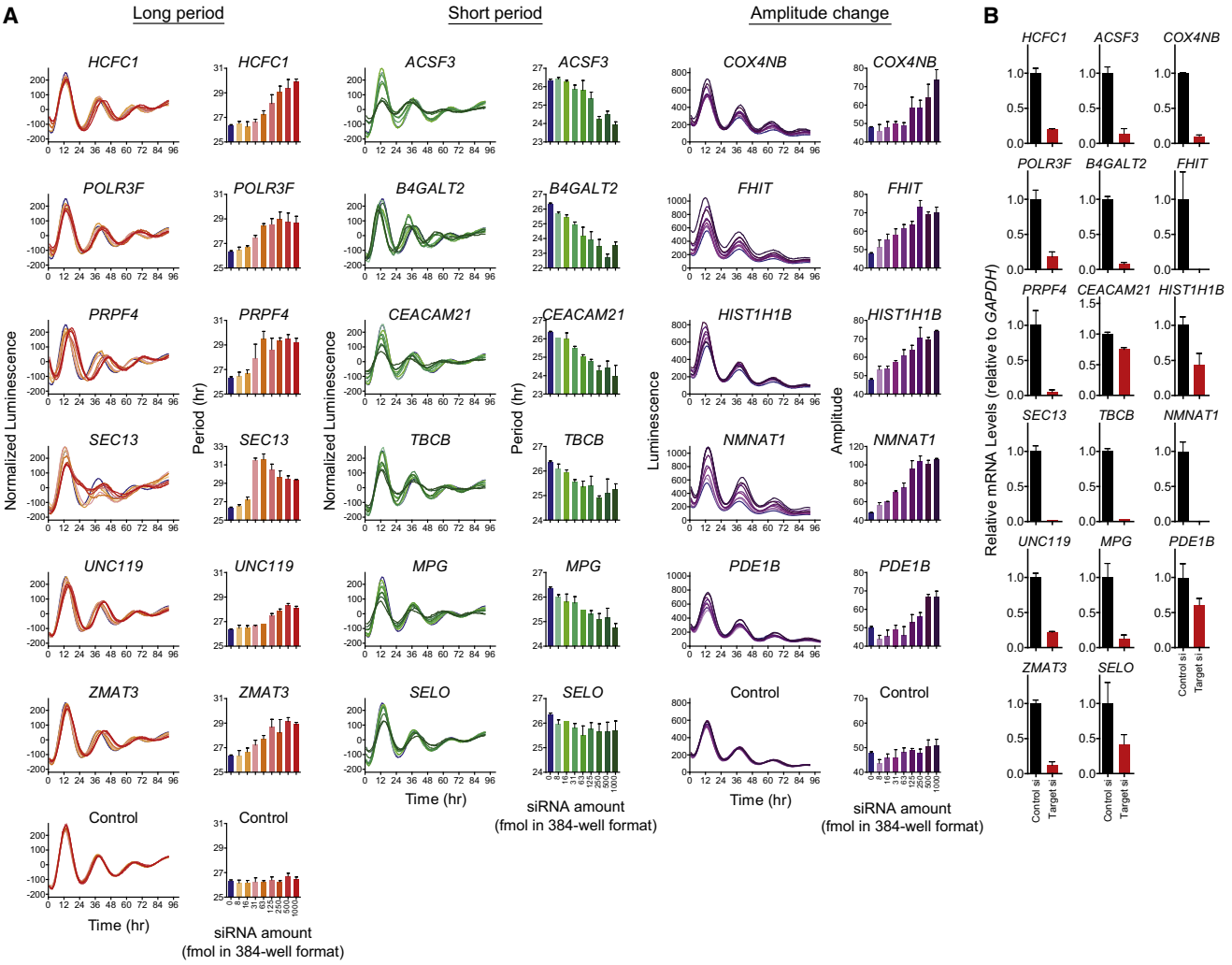

Figure 3. Dose-Dependent Phenotypic Validation

(A) Dose-dependent effects on circadian phenotypes. *Bmal1-dLuc* cells were transfected with the indicated amounts of siRNAs (eight-point, 2-fold dilution series; 8–1000 fmol/well) against 17 genes, and bioluminescence oscillations were recorded. Representative bioluminescence profiles (left) and circadian parameters (right) are indicated. Data represent the mean ± SD (n = 3).

(B) Knockdown of target genes. *Bmal1-dLuc* cells were transfected with 3000 fmol/well siRNAs (corresponding to 1000 fmol/well on 384-well plate) and subjected to Q-PCR analysis under unsynchronized conditions. mRNA levels of target genes relative to *GAPDH* are indicated. Data represent the mean ± SD (n = 2). In parallel experiments, bioluminescence rhythms were recorded and circadian phenotypes were confirmed.

screen impact clock function equivalently to or better than known clock components.

Dose-Dependent Effects on Clock Gene Expression

Because of the complex regulatory architecture of the clock gene network, perturbation of one clock component can lead to dynamic changes in the levels of others (we describe these as "network effects"). To determine whether genes from our screen had these effects, we selected a subset of genes that were confirmed in dose response (Figure 3): *POLR3F*, *PRPF4*, and *SEC13* (long-period hits), *ACSF3* and *MPG* (short-period hits), and *COX4NB* (high-amplitude hit) to analyze their potential for network effects. (The technical demands of this experiment prevented us from extending this analysis to all genes from Figure 3.) Knockdown of known clock genes had potent effects on circadian phenotypes, as well as clock gene expression (Figure 4), consistent with a previous study (Baggs et al., 2009). Interestingly, knockdown of most screen hits led to dose-dependent reduction of *NR1D1* and *DBP* transcript levels (Figure 4), consistent with E-box-driven regulation (Ueda et al., 2005; Liu et al., 2008; Baggs et al., 2009). These observations provide additional support for the notion that regulation of E-box-mediated transcription represents a topological vulnerability in mammalian circadian clocks (Ueda et al., 2005).

Similar to *NR1D1* knockdown, *SEC13* knockdown upregulated *BMAL1* transcription; like *NR1D1*, *SEC13* may impact clock function through network effects, rather than direct physical association with clock components. Intriguingly, knockdown

of *ACSF3* and *POLR3F* did not impact expression of core clock genes despite dose-dependent functional consequences on the clock (Figure 4). We note that *CRY2* knockdown also does not alter the messenger RNA (mRNA) levels of known clock genes. These genes may regulate posttranslational modification of clock components and impact protein abundance, localization, or function to perturb the oscillator.

Protein Interaction Network Analysis

We hypothesized that some hits from our screen directly or indirectly associate with known clock components. Using the Entrez Gene and Prolexys protein-protein interaction databases (Prolexys Pharmaceuticals, UT), we identified a comprehensive set of proteins that interacted with gene products of screen hits or known clock components (Table S2). To visualize the global topography of these interactions, we constructed an expanded clock gene interaction network (Figure 5). Most genes identified in our screen are present in a highly connected cluster of proteins centered on the core clock components: BMAL1, CLOCK, PERs, and CRYs. While ZMAT3, BLNK, and RRP12 directly interact with core clock components, most others associate indirectly through bridging molecules. (Many of these bridging molecules have phenotypic effects in our screen, but fell short of our reporting threshold.) For example, P53 (official name: TP53, tumor protein 53) physically interacts with CDK9, MAPK8, NCL, ABL1, BCR, DHFR, and BRCA2, as well as PCAF and CSNK1E; knockdown of these genes generate short-period, long-period, and high-amplitude phenotypes in our screen. Knockdown of *P53* itself generated low-amplitude rhythms in our screen; U2OS cells are wild-type for *P53* expression (Florenes et al., 1994). Interestingly, a recent RNAi screen showed that BMAL1 potently regulates P53 pathway function (Mullenders et al., 2009). Taken together, these observations provide evidence of the interconnectedness between the circadian clock and many other cellular pathways.

Pathway Analysis of Primary Screen Hits

Although the protein interaction network analysis gave some sense of pathway regulation, we sought to directly test for functional interconnectedness between the clock and other biological processes using the NIH DAVID pathway analysis tool (Huang et al., 2009; Dennis et al., 2003). We found that hits from our screen were members of dozens of cellular pathways. In addition, several pathways were overrepresented in this analysis, including insulin signaling ($p < 0.013$), hedgehog signaling ($p < 0.0088$), cell cycle ($p < 0.054$), and folate metabolism ($p < 0.014$) (Figures 6A and S5). While inhibition of multiple components of the insulin, hedgehog, or cell-cycle pathways resulted in long period length of circadian oscillations, knockdown of components of folate metabolism resulted in short- and long-period, as well as high-amplitude, phenotypes. (We note that components of these pathways often play important roles in other pathways; for example, several components in insulin signaling are shared in B cell receptor, IL-4, IL-8, PDGF, and IGF-1 signaling.) Our previous work has demonstrated that many components in these pathways are themselves under clock control and expressed in a circadian fashion in various peripheral tissues such as the liver (Panda et al., 2002a; Hughes et al., 2009). Collectively, these data show functional interconnectedness between the circadian clock and many other biological pathways.

One dramatic example of this regulation is the insulin signaling pathway (Figure 6A). (Insulin signaling and many other pathways have inherent feedback mechanisms; in this regard, these pathways may not function in a wholly cell-autonomous manner, and instead may autoregulate in *trans*.) Downregulation of multiple components of the insulin pathway resulted in period changes, including *JNK* (*MAPK8*, long period), *IKK* (*IKBKB*, long period), *PI3K* (*PIK3R5*, long period), *MTOR* (*FRAP1*, long period), *APKC* (*PRKCI*, long period), *PFK* (*PFKP*, short period), and *PYK* (*PKLR*, long period) (Figure 6B). In addition, at least 19 components of the insulin pathway are regulated at the transcriptional level by the circadian clock (Figure 6A). These include *IKK*, *PI3K*, and *MTOR*, whose perturbation also impacts clock function. To provide additional validation, we employed small molecules targeting multiple components of the insulin pathway in the U2OS model. SP600125 (a JNK inhibitor) and the Dequalinium analog C14 linker (a PKC inhibitor) led to long period length of circadian oscillations, PMA (a PKC activator) resulted in short period length, and wortmannin and LY294002 (PI3K inhibitors) resulted in a phase delay (Figure 6C). These results are all consistent with genetic perturbation of their intended targets. These results highlight the functional intersection between two important biological pathways, insulin signaling and the circadian clock.

Data Presentation in BioGPS

To facilitate use of this resource, we constructed a database to enable visualization and exploration. Our screening data are displayed as a plug-in in BioGPS, an open-access, searchable database for aggregating gene annotation from multiple online sources (http://biogps.gnf.org/). We created a custom BioGPS circadian layout focused on the siRNA screen described in this manuscript (Figure S6) and accessible at http://biogps.gnf.org/circadian/. This BioGPS layout displays plug-ins from our siRNA circadian screen and a recently published 1 hr resolution circadian gene expression databases from mouse liver and pituitary tissues (Hughes et al., 2009). Additional online resources are also available including the UCSC Genome Browser (http://genome.ucsc.edu/), our previously published reference gene expression data obtained from various tissues and cell lines (Su et al., 2002; Su et al., 2004), and Wikipedia, which describes the expanded gene annotations (e.g., *PER2* as shown here). Furthermore, BioGPS provides a flexible platform for building customized layouts that can be modified to include a selection of the more than 100 other online data sets and/or resources in the BioGPS plug-in library.

DISCUSSION

To identify additional clock genes or modulators, we carried out a genome-wide siRNA screen using a robust reporter gene assay in human U2OS cells. We found nearly 1000 genes whose knockdown resulted in low-amplitude circadian oscillations, which may indicate their potential in regulating the general health of cells. In addition, we found hundreds of genes whose

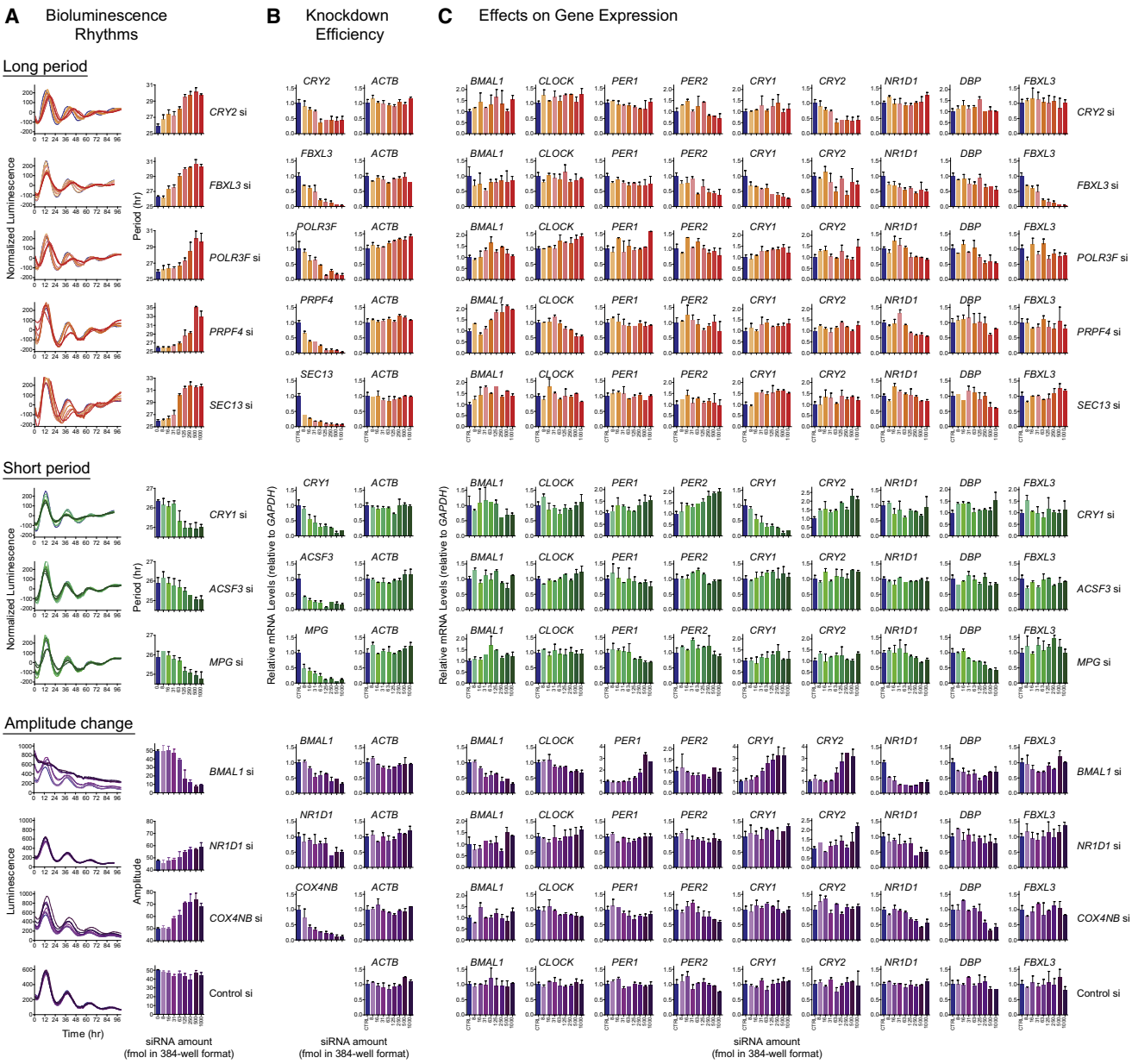

D

siRNA \ mRNA levels	BMAL1	CLOCK	PER1	PER2	CRY1	CRY2	NR1D1	DBP	FBXL3
CRY2						down			
FBXL3				down	down		down	down	down
POLR3F							down	down	
PRPF4	up	down					down	down	
SEC13	up				up			down	
CRY1	down			up	down	up			
ACSF3									
MPG			down				down	down	
BMAL1	down	down	up		up	up	down	down	
NR1D1	up					up	down		
COX4NB				down			down	down	

Figure 4. Dose-Dependent Effects of siRNAs on Clock Gene Expression

(A) Dose-dependent effects on circadian phenotype. *Bmal1-dLuc* cells were transfected with siRNAs (eight-point, 2-fold dilution series, 8–1000 fmol/well) designed against 11 genes including clock gene controls, and bioluminescence rhythms were recorded. Representative bioluminescence profiles (left) and circadian parameters (right) are indicated. Data represent the mean ± SD (n = 3).

(B and C) Dose-dependent knockdown of target genes (B) and effects on known clock gene expression (C). *Bmal1-dLuc* cells were transfected with siRNAs (eight-point, 2-fold dilution series, 24–3000 fmol/well) and analyzed by Q-PCR in unsynchronized conditions. mRNA levels of target gene (left) and *ACTB* (right,

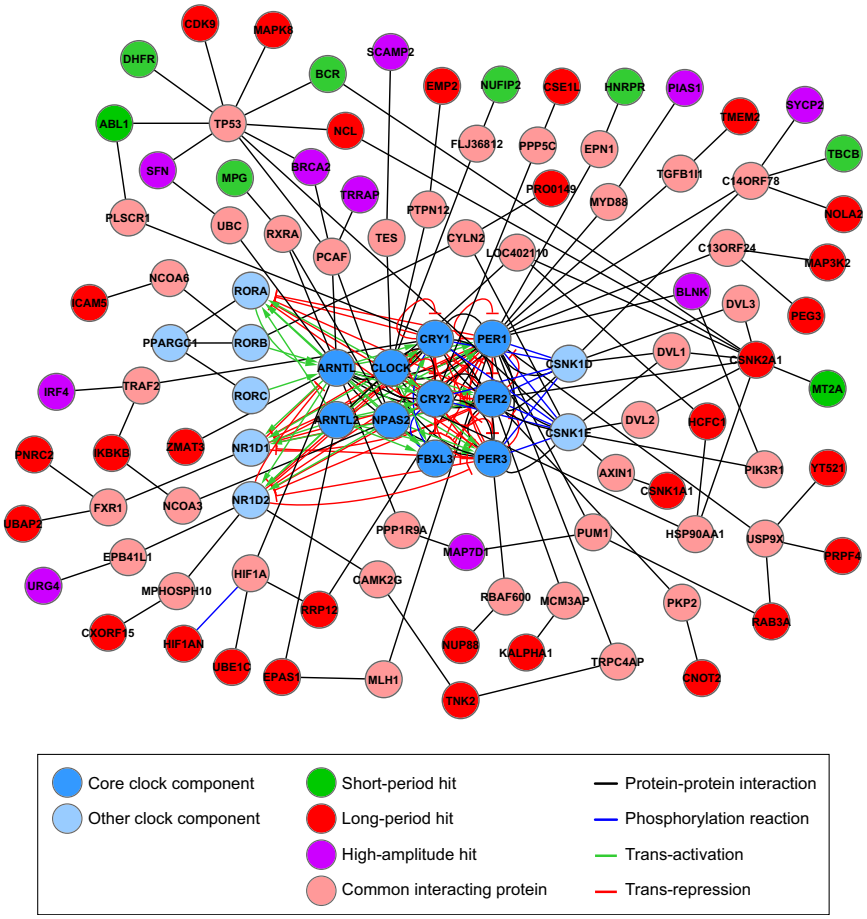

Figure 5. The Expanded Clock Gene Network

Clock components in the core feedback loop (blue), as well as other clock components known to regulate clock mechanism (light blue), were used to identify a list of interactors from the hits identified in the primary siRNA screen (green, short period; red, long period; purple, high amplitude) (Table S2). Protein-protein interactions were collated from Entrez Gene and the Prolexys protein-protein interaction databases. Common interacting proteins (pink) are depicted as nodes (circles). Edges are depicted as protein-protein interactions (black), phosphorylation reactions (blue), transactivation (green), and transrepression (red). The graph was generated in Cytoscape (http://www.cytoscape.org/).

knockdown led to long or short period length of oscillation or increased amplitude. Many of these factors had phenotypic effects on the oscillator similar to known clock components including dose-dependent perturbation. These genes are excellent points of intervention for perturbation of autonomous clock properties and may later prove important in regulation of physiology and behavior in the whole organism. Molecular analysis of these dose-dependent genes suggests that most of these genes function by regulating clock gene expression levels. These observations point the way to new aspects of genetic network architecture and possibly new feedback loops in the clock.

Protein interaction network analysis showed that some factors physically interact with core clock components, while others interact with bridging proteins that physically interact with the clock (one degree of separation). This analysis also showed that the P53 pathway is functionally interconnected with the clock. Focused pathway analysis of screen hits dramatically extend this observation—genes from dozens of pathways are represented on our hit list, and several pathways, including insulin and hedgehog signaling, the cell cycle, and folate metabolism, are overrepresented. Previous data has shown that these pathways are clock regulated. Collectively, we conclude the clock is massively interconnected and functionally intertwined with many biological pathways. As a cautionary note, observations from this cellular model may not be directly applicable to clock function in the whole organism as many genes identified in our screen are tissue specific.

Why is this interconnectedness important? Research in other fields has shown perturbation of one pathway often has deleterious and unintended consequences on another. For example, COX2 inhibitors such as Vioxx were designed to inhibit pain and inflammation; however, intermediates produced by COX2 (and inhibited by this class of small molecules) also afford cardio protection (FitzGerald, 2004). Alternatively, this interconnectedness may provide advantages—many of the above pathways have specific inhibitors that may prove useful in altering circadian phenotypes. Knowledge of this interconnectedness will be valuable in exploiting existing tools while avoiding the potentially deleterious consequences of doing so blindly.

Finally, we provide a publicly accessible resource to explore and visualize this data. It is our hope that this resource will serve as a useful launching point for colleagues studying the circadian clock in interpretation of their biochemical and genetic results to accelerate understanding of how the clock regulates physiology and behavior.

EXPERIMENTAL PROCEDURES

Materials

U2OS cells were obtained from the American Type Culture Collection (ATCC). We generated *Bmal1-dLuc* and *Per2-dLuc* reporter cell lines. The siRNA

as control) relative to *GAPDH* are indicated in (B), and mRNA levels of nine clock genes relative to *GAPDH* are indicated in (C). Data represent the mean ± SD (n = 2). In parallel experiments, bioluminescence rhythms were recorded and circadian phenotypes were confirmed.
(D) Summary of dose-dependent effects on known clock gene expression.

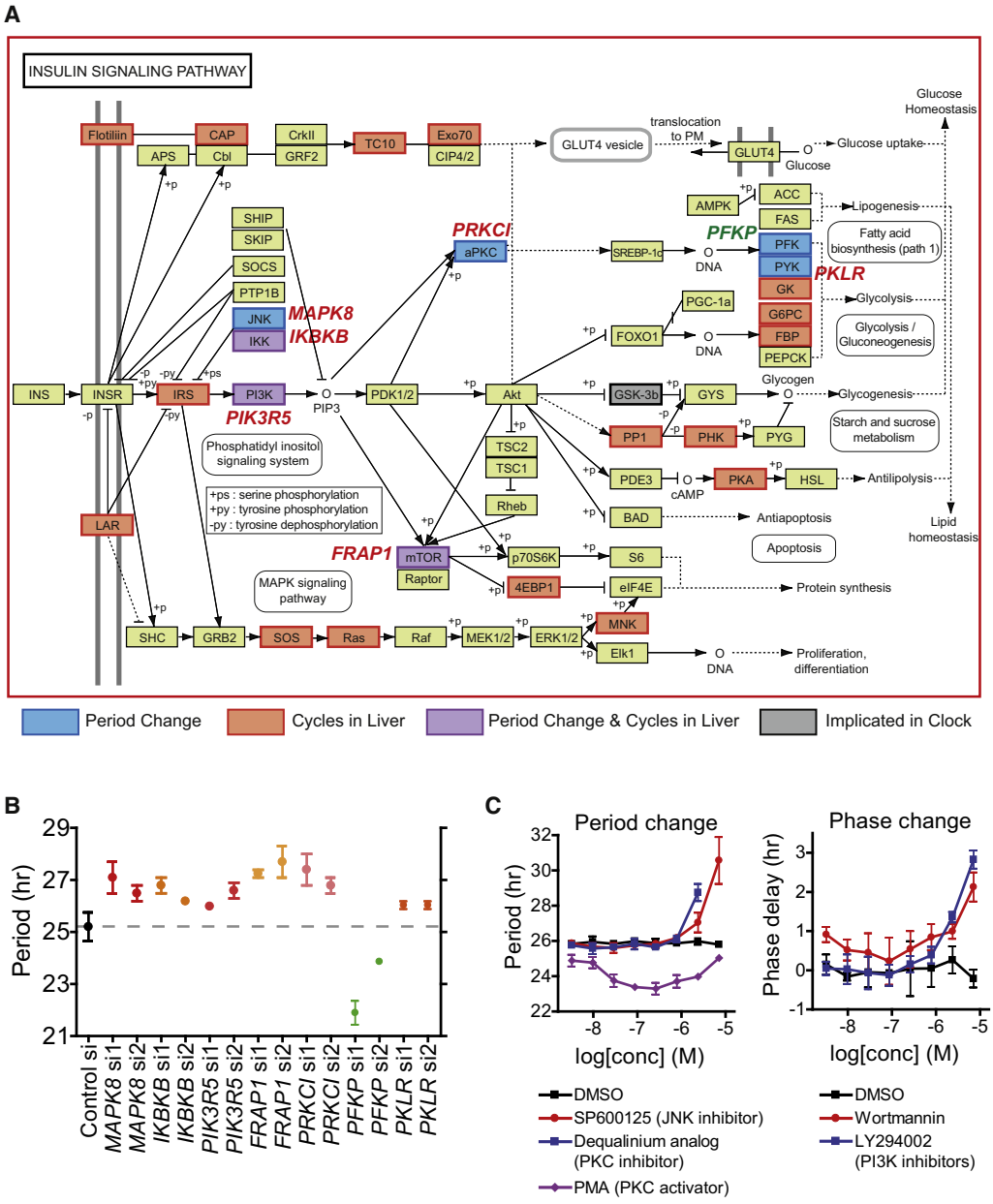

Figure 6. Regulation of Cellular Circadian Clock by Components in the Insulin Signaling Pathway

(A) Insulin signaling pathway genes that impact circadian function. Using the NIH DAVID Pathway Analysis tool, we identified many components of the insulin signaling pathway represented in our screen hits. Genes that impact clock function and genes regulated by the clock are indicated with colored boxes.

(B) Effects of siRNAs against genes involved in insulin signaling. The representative results from the secondary screen using individual siRNA are presented. Data represent the mean ± SD (n = 2).

(C) Effects of chemical inhibitors against protein kinases involved in insulin signaling. Bioluminescence rhythms of *Bmal1-dLuc* cells were monitored in the presence of various concentrations of compounds (eight points of 3-fold dilution series; final 3 nM–7 μM). Period or phase parameter was plotted against final concentrations of the compound. Data represent the mean ± SD (n = 4). The results for SP600215 and PMA are consistent with our previous observations (Hirota et al., 2008).

libraries used in the primary and secondary screens were purchased from QIAGEN. Additional siRNAs were purchased from Invitrogen and Dharmacon and used as controls in target validation experiments. GL2 and GL3 siRNAs designed against the *Luc* in pGL2 and pGL3 vectors, respectively, were purchased from QIAGEN. The GL2 siRNA was used as a negative control. Screen controls purchased from Invitrogen included *CRY1*-HSS102308, *CRY2*-HSS102311, and *BMAL1* or *ARNTL*-HSS100703. *CRY1* and *NR1D1* siRNAs used in dose-dependent experiment were previously described (Baggs et al., 2009). Other siRNAs used in the dose experiment are listed in Table S3 and were used as pools.

Cell Line Establishment

U2OS cells were grown in regular Dulbecco's modified Eagle's medium (DMEM) supplemented with 10% fetal bovine serum (FBS) and antibiotics.

Lentiviral *Per2-dLuc* and *Bmal1-dLuc* reporters (Liu et al., 2008) were introduced into U2OS cells via lentivirus-mediated infection as described (Liu et al., 2008). We selected stable cell lines with blasticidin and clonal lines by fluorescence-activated cell sorting (FACS)-based single-cell sorting in 96-well plates; we tested these lines as described in the LumiCycle (Liu et al., 2008). The clonal lines are genetically and morphologically indistinguishable from parental cells and represent the average period length of the infected cell population.

Transfection and ViewLux Recording

For primary siRNA screens, U2OS circadian reporter cells were reverse transfected with siRNAs in 384-well plates. In brief, we trypsinized rapidly growing cells and resuspended them in DMEM containing 20% FBS without antibiotics at 0.1 × 10^6 cells/ml. We next added 20 μl of transfection reagent mixture (3.3 μl/ml or 0.066 μl/well Lipofectamine 2000 in Opti-MEM) to each well containing prespotted siRNA constructs (1 pmol; 0.5 pmol for each siRNA; final concentration of 12.5 nM), incubated them at room temperature for 20 min, and added 20 μl of cells (2000 cells/well) with our robotic system. Approximately 18 hr after transfection, we replaced this media with 60 μl prewarmed fresh DMEM containing 10% FBS and antibiotics and allowed the cells to grow for an additional 2 days.

Three days after transfection, we replaced this media with 60 μl HEPES-buffered explant medium supplemented with luciferin (1 μM) (Promega) and B-27 supplements (Invitrogen), and the plates were sealed with an optically clear film (USA Scientific). We next loaded these plates in a 36°C incubator and recorded bioluminescence expression with a ViewLux (Perkin Elmer). We measured bioluminescence for 30 s every 2 hr for 4 days. Secondary screens were performed in the same manner. For technical reasons, 20 out of the 292 plates in the primary screen were recorded for 3 days.

Data Mining

The primary screen produced a total of >4.3 × 10^6 data points (Tables S4 and S5). We used the MultiCycle circadian data analysis program (Actimetrics) to analyze recorded bioluminescence data. In brief, data was detrended by subtraction of a best fit line (first order polynomial) and, subsequently, were fit to a sine wave to obtain circadian parameters such as rhythm period length and amplitude.

Mechanistic Validation

The *Bmal1-dLuc* cells were transfected as described (Hirota et al., 2008) with a small modification, 0.4 μl/well of Lipofectamine 2000. Parallel transfection experiments were performed for Q-PCR and functional analyses. For Q-PCR analysis, the cells were harvested prior to medium change for rhythm recording and therefore unsynchronized. Total RNA preparation and Q-PCR were performed as described (Hirota et al., 2008). SYBR Green PCR Master Mix (Applied Biosystems) or QuantiTect SYBR Green PCR kit (QIAGEN) was used for Q-PCR. The primers used in Q-PCR analysis are listed in Table S4.

ACCESSION NUMBER

The primary screening data reported in this paper has been deposited in the PubChem Bioassay database of the National Center for Biotechnology Information with the accession number AID 1904.

SUPPLEMENTAL DATA

Supplemental Data include six figures and six tables and can be found with this article online at http://www.cell.com/supplemental/S0092-8674(09)01099-X.

ACKNOWLEDGMENTS

We thank Buu Tu for technical support in the screens, Jia Zhang and Tony Orth for help with Qiagen siRNA libraries, Chunlei Wu and Ghislain Bonamy for help with BioGPS, and Richard Glynne and Peter Schultz for their institutional support and encouragement. We also thank Jose Pruneda-Paz, Elizabeth Hamilton, Dmitri A. Nusinow, Michael Hughes, Julie Baggs, and Jason DeBruyne for critically reading the manuscript. This work is supported by National Institutes of Health grants to S.A.K. (MH51573 and GM74868). J.B.H. is supported by the Pennsylvania Commonwealth Health Research Formula Funds, the National Institute of Neurological Disease and Stroke (1R01NS054794), and the National Institute of Mental Health (P50 MH074924-01, awarded to Joseph S. Takahashi, Northwestern University). A.C.L. is supported by The University of Memphis startup fund and the National Science Foundation (IOS-0920417). S.A.K. is a founder of ReSet Therapeutics and is a member of its Scientific Advisory Board. BioGPS development is supported by NIGMS (1R01GM083924 to A.I.S.). This is manuscript number 090513 of the Genomics Institute of the Novartis Research Foundation.

Received: May 30, 2009
Revised: July 3, 2009
Accepted: August 20, 2009
Published online: September 17, 2009

REFERENCES

Andre, E., Conquet, F., Steinmayr, M., Stratton, S.C., Porciatti, V., and Becker-Andre, M. (1998). Disruption of retinoid-related orphan receptor beta changes circadian behavior, causes retinal degeneration and leads to vacillans phenotype in mice. EMBO J. *17*, 3867–3877.

Aza-Blanc, P., Cooper, C.L., Wagner, K., Batalov, S., Deveraux, Q.L., and Cooke, M.P. (2003). Identification of modulators of TRAIL-induced apoptosis via RNAi-based phenotypic screening. Mol. Cell *12*, 627–637.

Baggs, J.E., Price, T.S., DiTacchio, L., Panda, S., FitzGerald, G.A., and Hogenesch, J.B. (2009). Network features of the mammalian circadian clock. PLoS Biol. *7*, e52.

Balsalobre, A., Damiola, F., and Schibler, U. (1998). A serum shock induces circadian gene expression in mammalian tissue culture cells. Cell *93*, 929–937.

Brown, S.A., Fleury-Olela, F., Nagoshi, E., Hauser, C., Juge, C., Meier, C.A., Chicheportiche, R., Dayer, J.M., Albrecht, U., and Schibler, U. (2005). The period length of fibroblast circadian gene expression varies widely among human individuals. PLoS Biol. *3*, e338.

Busino, L., Bassermann, F., Maiolica, A., Lee, C., Nolan, P.M., Godinho, S.I.H., Draetta, G.F., and Pagano, M. (2007). SCFFbxl3 controls the oscillation of the circadian clock by directing the degradation of cryptochrome proteins. Science *316*, 900–904.

Conkright, M.D., Guzman, E., Flechner, L., Su, A.I., Hogenesch, J.B., and Montminy, M. (2003). Genome-wide analysis of CREB target genes reveals a core promoter requirement for cAMP responsiveness. Mol. Cell *11*, 1101–1108.

DeBruyne, J.P., Noton, E., Lambert, C.M., Maywood, E.S., Weaver, D.R., and Reppert, S.M. (2006). A clock shock: mouse CLOCK is not required for circadian oscillator function. Neuron *50*, 465–477.

DeBruyne, J.P., Weaver, D.R., and Reppert, S.M. (2007). Peripheral circadian oscillators require CLOCK. Curr. Biol. *17*, R538–R539.

Dennis, G., Jr., Sherman, B.T., Hosack, D.A., Yang, J., Gao, W., Lane, H.C., and Lempicki, R.A. (2003). DAVID: Database for Annotation, Visualization, and Integrated Discovery. Genome Biol. *4*, 3.

Echeverri, C.J., Beachy, P.A., Baum, B., Boutros, M., Buchholz, F., Chanda, S.K., Downward, J., Ellenberg, J., Fraser, A.G., Hacohen, N., et al. (2006). Minimizing the risk of reporting false positives in large-scale RNAi screens. Nat. Methods *3*, 777–779.

Etchegaray, J.P., Machida, K.K., Noton, E., Constance, C.M., Dallmann, R., Di Napoli, M.N., DeBruyne, J.P., Lambert, C.M., Yu, E.A., Reppert, S.M., and Weaver, D.R. (2009). Casein kinase 1 delta regulates the pace of the mammalian circadian clock. Mol. Cell. Biol. *29*, 3853–3866.

FitzGerald, G.A. (2004). Coxibs and cardiovascular disease. N. Engl. J. Med. *351*, 1709–1711.

Florenes, V.A., Maelandsmo, G.M., Forus, A., Andreassen, A., Myklebost, O., and Fodstad, O. (1994). MDM2 gene amplification and transcript levels in

human sarcomas: relationship to TP53 gene status. J. Natl. Cancer Inst. *86*, 1297–1302.

Gachon, F., Fleury-Olela, F., Schaad, O., Descombes, P., and Schibler, U. (2006). The circadian PAR-domain basic leucine zipper transcription factors DBP, TEF, and HLF modulate basal and inducible xenobiotic detoxcification. Cell Metab. *4*, 25–36.

Gallego, M., and Virshup, D.M. (2007). Post-translational modifications relgulate the ticking of the circadian clock. Nat. Rev. Mol. Cell Biol. *8*, 139–148.

Godinho, S.I., Maywood, E.S., Shaw, L., Tucci, V., Barnard, A.R., Busino, L., Pagano, M., Kendall, R., Quwailid, M.M., Romero, M.R., et al. (2007). The after-hours mutant reveals a role for Fbxl3 in determining mammalian circadian period. Science *316*, 897–900.

Hirota, T., Lewis, W.G., Liu, A.C., Lee, J.W., Schultz, P.G., and Kay, S.A. (2008). A chemical biology approach reveals period shortening of the mammalian circadian clock by specific inhibition of GSK-3{beta}. Proc. Natl. Acad. Sci. USA *105*, 20746–20751.

Huang, d.W., Sherman, B.T., and Lempicki, R.A. (2009). Systematic and integrative analysis of large gene lists using DAVID bioinformatics resources. Nat. Protocols *4*, 44–57.

Hughes, M.E., DiTacchio, L., Hayes, K.R., Vollmers, C., Pulivarthy, S., Baggs, J.E., Panda, S., and Hogenesch, J.B. (2009). Harmonics of circadian gene transcription in mammals. PLoS Genet. *5*, e1000442.

Iourgenko, V., Zhang, W., Mickanin, C., Daly, I., Jiang, C., Hexham, J.M., Orth, A.P., Miraglia, L., Meltzer, J., Garza, D., et al. (2003). Identification of a family of cAMP response element-binding protein coactivators by genome-scale functional analysis in mammalian cells. Proc. Natl. Acad. Sci. USA *100*, 12147–12152.

Liu, A.C., Lewis, W.G., and Kay, S.A. (2007a). Mammalian circadian signaling networks and therapeutic targets. Nat. Chem. Biol. *3*, 631–639.

Liu, A.C., Welsh, D.K., Ko, C.H., Tran, H.G., Zhang, E.E., Priest, A.A., Buhr, E.D., Singer, O., Meeker, K., Verma, I.M., et al. (2007b). Intercellular coupling confers robustness against mutations in the SCN circadian clock network. Cell *129*, 605–616.

Liu, C., Li, S., Liu, T., Borjigin, J., and Lin, J.D. (2007c). Transcriptional coactivator PGC-1alpha integrates the mammalian clock and energy metabolism. Nature *447*, 477–481.

Liu, A.C., Tran, H.G., Zhang, E.E., Priest, A.A., Welsh, D.K., and Kay, S.A. (2008). Redundant function of REV-ERBalpha and beta and non-essential role for Bmal1 cycling in transcriptional regulation of intracellular circadian rhythms. PLoS Genet. *4*, e1000023.

Maier, B., Wendt, S., Vanselow, J.T., Wallach, T., Reischl, S., Oehmke, S., Schlosser, A., and Kramer, A. (2009). A large-scale functional RNAi screen reveals a role for CK2 in the mammalian circadian clock. Genes Dev. *23*, 708–718.

Meng, Q.J., Logunova, L., Maywood, E.S., Gallego, M., Lebiecki, J., Brown, T.M., Sladek, M., Semikhodskii, A.S., Glossop, N.R., Piggins, H.D., et al. (2008). Setting clock speed in mammals: the CK1 epsilon tau mutation in mice accelerates circadian pacemakers by selectively destabilizing PERIOD proteins. Neuron *58*, 78–88.

Mullenders, J., Fabius, A.W., Madiredjo, M., Bernards, R., and Beijersbergen, R.L. (2009). A large scale shRNA barcode screen identifies the circadian clock component ARNTL as putative regulator of the p53 tumor suppressor pathway. PLoS ONE *4*, e4798.

Panda, S., Antoch, M.P., Miller, B.H., Su, A.I., Schook, A.B., Straume, M., Schultz, P.G., Kay, S.A., Takahashi, J.S., and Hogenesch, J.B. (2002a). Coordinated transcription of key pathways in the mouse by the circadian clock. Cell *109*, 307–320.

Panda, S., Hogenesch, J.B., and Kay, S.A. (2002b). Circadian rhythms from flies to human. Nature *417*, 329–335.

Preitner, N., Damiola, F., Molina, L.L., Zakany, J., Duboule, D., Albrecht, U., and Schibler, U. (2002). The orphan nuclear receptor REV-ERB alpha controls circadian transcription within the positive limb of the mammalian circadian oscillator. Cell *110*, 251–260.

Reddy, A.B., Karp, N.A., Maywood, E.S., Sage, E.A., Deery, M., O'Neill, J.S., Wong, G.K., Chesham, J., Odell, M., Lilley, K.S., et al. (2006). Circadian orchestration of the hepatic proteome. Curr. Biol. *16*, 1107–1115.

Reppert, S.M., and Weaver, D.R. (2002). Coordination of circadian timing in mammals. Nature *418*, 935–941.

Sato, T.K., Panda, S., Miraglia, L.J., Reyes, T.M., Rudic, R.D., McNamara, P., Naik, K.A., FitzGerald, G.A., Kay, S.A., and Hogenesch, J.B. (2004). A functional genomics strategy reveals Rora as a component of the mammalian circadian clock. Neuron *43*, 527–537.

Siepka, S.M., Yoo, S.H., Park, J., Song, W., Kumar, V., Hu, Y., Lee, C., and Takahashi, J.S. (2007). The circadian mutant Overtime reveals F-box protein FBXL3 regulation of cryprochrome and period gene expression. Cell *129*, 1011–1023.

Su, A.I., Cooke, M.P., Ching, K.A., Hakak, Y., Walker, J.R., Wiltshire, T., Orth, A.P., Vega, R.G., Sapinoso, L.M., Moqrich, A., et al. (2002). Large-scale analysis of the human and mouse transcriptomes. Proc. Natl. Acad. Sci. USA *99*, 4465–4470.

Su, A.I., Wiltshire, T., Batalov, S., Lapp, H., Ching, K.A., Block, D., Zhang, J., Soden, R., Hayakawa, M., Kreiman, G., et al. (2004). A gene atlas of the mouse and human protein-encoding transcriptomes. Proc. Natl. Acad. Sci. USA *101*, 6062–6067.

Takahashi, J.S. (2004). Finding new clock components: past and future. J. Biol. Rhythms *19*, 339–347.

Ueda, H.R., Chen, W.B., Adachi, A., Wakamatsu, H., Hayashi, S., Takasugi, T., Nagano, M., Nakahama, K., Suzuki, Y., Sugano, S., et al. (2002). A transcription factor response element for gene expression during circadian night. Nature *418*, 534–539.

Ueda, H.R., Hayashi, S., Chen, W.B., Sano, M., Machida, M., Shigeyoshi, Y., Iino, M., and Hashimoto, S. (2005). System-level identification of transcriptional circuits underlying mammalian circadian clocks. Nat. Genet. *37*, 187–192.

Ukai-Tadenuma, M., Kasukawa, T., and Ueda, H.R. (2008). Proof-by-synthesis of the transcriptional logic of mammalian circadian clocks. Nat. Cell Biol. *10*, 1154–1163.

Vanselow, K., Vanselow, J.T., Westermark, P.O., Reischl, S., Maier, B., Korte, T., Herrmann, A., Herzel, H., Schlosser, A., and Kramer, A. (2006). Differential effects of PER2 phosphorylation: molecular basis for the human familial advanced sleep phase syndrome (FASPS). Genes Dev. *20*, 2660–2672.

Xu, Y., Padiath, Q.S., Shapiro, R.E., Jones, C.R., Wu, S.C., Saigoh, K., Ptacek, L.J., and Fu, Y.H. (2005). Functional consequences of a CKI delta mutation causing familial advanced sleep phase syndrome. Nature *434*, 640–644.